

### **Nemanja Markovic**

Assistant, Dipl.–Ing.

Faculty of Civil Engineering and Architecture  
University of Nis, Serbia

nemanja.markovic@gaf.ni.ac.rs

### **Dragoslav Stojic**

Dr.-Ing., Full Professor

Faculty of Civil Engineering and Architecture  
University of Nis, Serbia

dragoslav.stojic@gmail.com

### **Tamara Nestorovic**

Dr.-Ing., Full Professor

Faculty of Civil and Environmental  
Engineering, Ruhr University Bochum,  
Germany

tamara.nestorovic@rub.de

## **NUMERICAL MODELING OF PIEZOELECTRIC SMART AGGREGATES**

The article deals with numerical modeling of piezoelectric smart aggregates based on finite element method. Finite element modeling of piezoelectric patch is based on constitutive equations for coupled electro-mechanical behavior, while for surrounding concrete linear elastic material model is assumed. Different intensities of electric voltage were analyzed and displacements at control points were measured. Obtained results indicate that there is a complete linear relationship between the deformation and the electrical voltage at the control points, and nonlinear development of deformation by cross-sectional thickness of piezoelectric smart aggregate.

**Keywords:** Piezoelectricity, Smart Aggregates, ABAQUS, Finite Element Method, Structural Health Monitoring.

### **1. INTRODUCTION**

Structural health monitoring and damage detection of reinforced concrete structures using piezoelectric actuators/sensors has become possible and practicable after piezoelectric smart aggregates (PZT SA) were developed. Multifunctional smart sensors, called PZT SA were developed at the University of Houston, USA. Since then, numerous researches have been conducted, aimed at the potential implementation of PZT SA for damage detection and monitoring in RC structures in real-time or near real-time. The goal of the developed methods and procedures for detection, localization and quantification of damage is acquisition of a sufficient number of reliable data on whose basis a decision of further interventions could be made. Further interventions (assuming the detection found damage in the structure) comprise making decisions on the visual inspection, potential detailed structural examination to serve as a basis for making a definitive decision on the rehabilitation, reconstruction or demolition of the structure. The paper is organized as follows: after the introduction, the description and application of PZT SA are presented in Section 2. Numerical simulation of PZT SA based on FEM is presented in Section 3, while the results and discussions are presented in Section 4.

Finally, conclusions and recommendations for further investigations are given in Section 5.

## 2. PIEZOELECTRIC SMART AGGREGATES

A lead zirconate titanate (PZT) patch, protected by a waterproof layer and embedded in a very small concrete block, marble or rock represents PZT SA. *Piezoelectric Smart Aggregate* got its name because: **Piezoelectric** – because it contains a patch with piezoelectric properties (effects), **Smart** – because it has smart characteristics and a multifunctional character, **Aggregate** – because it is embedded in a small concrete blocks of ordinary size which is within the boundaries of the real aggregate size of  $16 \div 31,5 \text{ mm}$ . The fabricating process PZT SA mainly consists of the following steps: a) selection of the size and shape of a PZT patch, b) soldering of an electric cable to the PZT patch, c) connecting of the electric cable to BNC connector, d) waterproofing of PZT patch, e) mixing of cement paste, f) making of formwork, g) lubrication of formwork for easy demolding, h) fixing of the PZT patch in the formwork, i) pouring of fresh cement paste, j) curing for 48h and k) demolding of PZT SA from the formwork. In addition to embedding the PZT patches into cement paste, patches can be embedded in small marble blocks (Fig. 1) or blocks of other types of rocks.

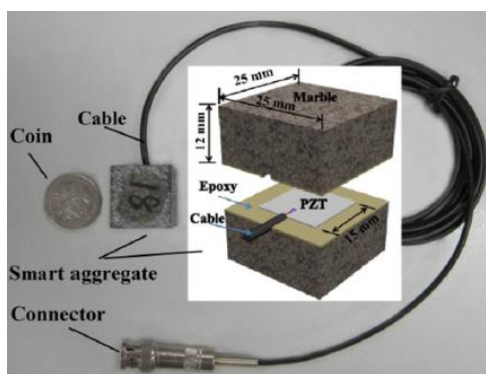


Figure 1. Marble PZT SA [1]

PZT patches are characterized by high brittleness and lack of resistance to moisture because of which they were unsuitable for usage in construction engineering. PZT SA protects the PZT patch from moisture and mechanical shocks during pouring of fresh concrete and during the building service. PZT SA is installed into a real structure by fixing it to the reinforcement bars (Fig. 2b, Fig. 2c) or formwork (Fig. 2a) at a predefined point. While installing it very important to ensure that

position and orientation of PZT SA does not change during pouring of fresh concrete mass.

After installing PZT SA in RC structures, damage detection is usually performed by the signal generator device for generation of sweep sinusoidal/harmonic/pulse voltage signals. This voltage signal is further amplified using power amplifier to drive the PZT SA actuator embedded in an RC structure. Spatial elastic waves propagate through an RC structure as a consequence of activation of the PZT SA actuator, using an inverse piezoelectric effect. On the other hand, the other PZT SA is used as sensor to receive of the incoming wave and for converting it into a voltage signal based on the direct piezoelectric effect. Finally, this output sensor signal is transferred to the storage device. This is a brief description of the procedure and equipment used for damage detection of RC structures using PZT SA.

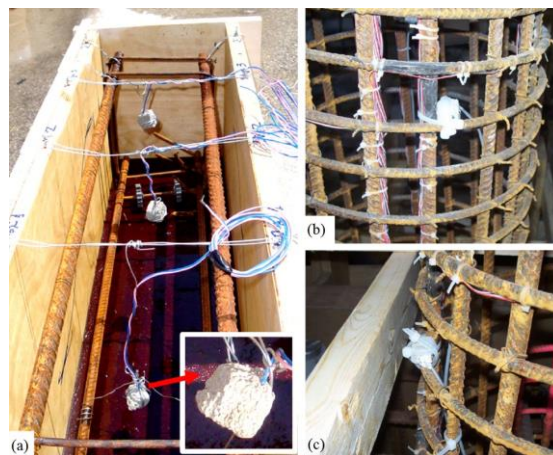


Figure 2. Fixing PZT SA inside structural elements: a) installation of PZT SA inside the wooden formwork of RC beam [2], b-c) A PZT SA fixed on the rebar cage of column [3]

Usage of PZT SA for damage detection has been analyzed for different cases of damage, different structural elements, loading cases, etc. In the laboratory conditions, damage detection based on the energy approach and one-dimensional damage index was performed for beam elements [4]. Beam loading was performed using hydraulic press and onset of cracks their propagation was monitored [5]. It was concluded that the implemented damage detection procedure can detect damage, but in-detail information on the cracks, such as their location, dimensions (width, length), orientation, cannot be established using this procedure [6]. Also, monitoring of RC walls under pseudo-static load, up to the gradual onset of first cracks, and further to failure was performed using PZT SA [7]. Similar to the previous research, the



with the following notation:  $\sigma_{ij}$ ,  $\varepsilon_{kl}$  - mechanical stress and strain tensor;  $q_i$  - electric “displacement” vector;  $D_{ijkl}^E$  - materials’ elastic stiffness matrix defined at zero electrical potential gradient;  $e_{mij}^\varphi$  - material’s piezoelectric stress coefficient matrix,  $d_{mij}^\varphi$  - material’s piezoelectric strain coefficient matrix;  $\varphi$  – electrical potential;  $D_{ij}^{\varphi(\sigma)}$  - material’s dielectric property;  $E_j$  - electric potential gradient vector.

A PZT patch responds to an electric potential gradient by mechanical straining (actuation effect), while the mechanical stress causes an electric potential gradient in the material (sensor effect). This coupling between the electric potential gradient and the strain is the material’s piezoelectric properties. When modeling PZT SA only the first piezoelectric effect was used – actuation effect (equation 3 and 4). Based on equation (3 and 4), it is obvious that electrical and electro-mechanical coupling behaviors are defined by the dielectric property  $D_{ij}^{\varphi(\sigma)}$  and the piezoelectric strain coefficient matrix  $d_{mij}^\varphi$ . PZT patch in this analysis is mechanically treated as linear-elastic model.

The mechanical equilibrium equation and electrical flux conservation equation for piezoelectric FEM analysis are:

$$\int_V \sigma : \delta \varepsilon \cdot dV = \int_S t \cdot \delta u \cdot dS + \int_V f \cdot \delta u \cdot dV \quad (5)$$

$$\int_V q \cdot \delta E \cdot dV = \int_S q_s \cdot \delta \varphi \cdot dS + \int_V q_v \cdot \delta \varphi \cdot dV \quad (6)$$

where  $\sigma$  is the Cauchy stress at a current point;  $t$  is the traction across a point of the surface of the body;  $f$  is the body force per unit volume in the node;  $\delta u$  is the virtual velocity field;  $\delta \varepsilon = sym(\partial \delta u / \partial x)$ ;  $q$  is the electric flux vector (electric “displacement” vector);  $q_s$  is the electric flux per unit area entering the body at a point on its surface;  $q_v$  is the electric flux entering the body per unit volume;  $\delta \varphi$  is the virtual potential and  $\delta E = -\partial \delta \varphi / \partial x$ .

Electric potentials and displacement for the piezoelectric elements exist at the nodal locations and they are approximated with interpolation functions:

$$u = N^N u^N, \quad \varphi = N^N \varphi^N \quad (7)$$

where  $u^N$ ,  $\varphi^N$  are nodal quantities and  $N^N$  is the array of interpolation functions. The electrical potential gradient and strains are given with next equation:

$$E = -B_\varphi^N \varphi^N, \quad \varepsilon = B_u^N u^N \quad (8)$$

where  $B_u^N$  and  $B_\varphi^N$  are the spatial derivatives of  $N^N$ , defined in the current configuration for geometrically nonlinear analysis. The following system of equations is derived in terms of nodal quantities:

$$M^{MN} \ddot{u}^N + K_{uu}^{MN} u^N + K_{\varphi u}^{MN} \varphi^N = P^M \quad (9)$$

$$K_{\varphi u}^{MN} \varphi^N - K_{\varphi \varphi}^{MN} \varphi^N = -Q^M \quad (10)$$

with following notation:  $M^{MN}$  - mass matrix;  $K_{uu}^{MN}$  - displacement stiffness matrix;  $K_{\varphi \varphi}^{MN}$  - dielectric “stiffness” matrix;  $K_{\varphi u}^{MN}$  - piezoelectric coupling matrix;  $P^M$  - mechanical force vector;  $Q^M$  - electrical charge vector.

Table 1. Material properties of PZT patch and concrete block (density in kg/m<sup>3</sup>)

Piezoelectric patch			
Density	Dielectric properties (CV <sup>-1</sup> /m)		
$\rho=7500$	$D_{11}=1.505$	$D_{22}=1.301$	$D_{33}=1.505$
Piezoelectric properties (F/m) · 10 <sup>-10</sup>			
$d_{112}=7.41, d_{211}=-2.74, d_{222}=5.93, d_{233}=-2.74,$ $d_{323}=7.41, d_{111}= d_{122}= d_{133}= d_{113}= d_{123}= d_{212}=0$ $d_{213}= d_{223}= d_{311}= d_{322}= d_{333}= d_{312}= d_{323}=0$			
Elastic properties (E and G in GPa)			
$E_1=E_3=60.61; E_2=48.31; G_{12}=G_{23}=23.0;$ $G_{13}=23.5; \nu_{12}=0.512; \nu_{13}=0.289; \nu_{23}=0.408;$			
Concrete block			
Young’s Modulus: $E=44.3$ GPa			
Poisson’s ratio: $\nu=0.15$			
Mass density: $\rho=2400$ kg/m <sup>3</sup>			
Rayleigh damping			
$\alpha=2050.0$		$\beta=1.100 \cdot 10^{-8}$	

The surrounding concrete block is modeled as a linear elastic isotropic material with material characteristics defined in table 1. The contact between the patch and the concrete block is defined by surface based tie constraints, simulating a complete connection between these



two parts. Piezoelectric contact surface was selected as a “master surface” and concrete contact surface was “slave surface”. Boundary condition on the concrete block are defined to external edge points by constrained all degrees of freedom. On one side of the PZT patch electric voltage equal to zero is fixed using the electric potential boundary condition, while on the other side is applied an electrical voltage having values ranging between 10V-100V with a step of 10V. The finite element mesh is made using the sweep technique of mesh generation with the approximate size of finite element of 0.03mm. The finite element used for modeling of the concrete block is the standard-linear-3D stress FE: C3D8R – 8-node linear brick with reduced integration and hourglass control. Whereas, for modeling of the PZT patch the standard-linear-piezoelectric FE: C3D8E – 8-node linear piezoelectric brick is used. Full analysis with multiple processors parallelization and single nodal output precision is performed. In the control points presented in Fig. 4, displacements in z-directions for all intermediate steps of the applied electric voltage are measured.

#### 4. RESULTS AND DISCUSSION

The results obtained based on the FEM analysis of PZT SA are presented in figures 4-6. In figures 5-6 displacements obtained in control points in the function of the applied electric voltage are presented. A clear linear dependence between the electric voltage and obtained displacements can be observed (Figure 5).

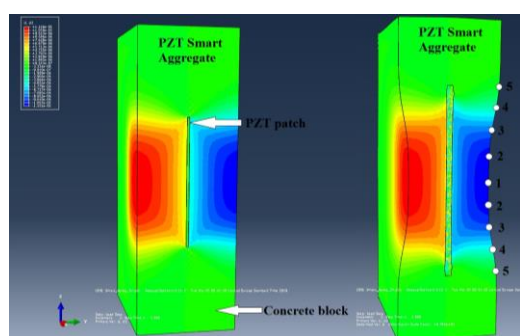


Figure 4. Left: Undeformed PZT SA model, Right: deformed PZT SA from ABAQUS/STANDARD

Figure 5 shows the values of the displacement  $U_z$  (displacement perpendicular to PZT transducer surface) for all control points for values of electrical voltage from 10V to 100V. As can be clearly seen, for the center point 1 the largest displacements are obtained, and they decrease nonlinearly to the point 5. The linear displacement-electric charge ratio

obtained in Figure 5 is the expected result since in ABAQUS there is a linear relationship between the electrical charge and the deformation of the PZT transducers. Also, the highest displacements are obtained in the control point 1 and they reduce non-linearly towards the point 5, which can more clearly be seen in figure 6. Measured displacements on the non-deformed model is presented in figure 4 left, while in figure 4 right are presented the same displacements on the deformed model.

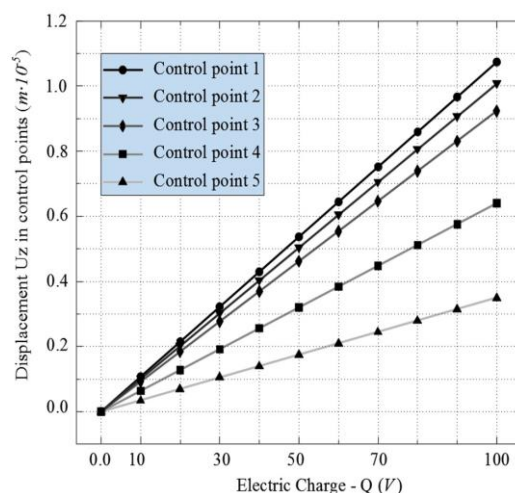


Figure 5. Results of displacement  $U_z$  in control points in function of electric charge (Q)

Displacements in the control points based on the FEM model done in the ABAQUS/ STANDARD software is presented in cross-section of PZT SA (Figure 6). Displacements are displayed in the function of the electrical voltage. Based on this figure, it can be seen that with the increase of the electrical voltage, deformations of PZT SA also increase. The assumption is made that at the ends of the cross-section the deformations are equal to zero. The results obtained from this model can be used for modeling of wave propagation induced by a PZT SA actuators. Such method of modeling can be implemented because there are no piezoelectric finite elements in the explicit FEM analysis in ABAQUS, and it is impossible to model wave propagation in the standard FEM analysis because of the excessive size of the model. For that reason, instead of PZT SA actuator, in the modeling of wave propagation, displacement boundary conditions can be used [14]. The excitation of concrete structures by the PZT actuators, and causing ultrasonic wave propagation inside the structure, occurs due to deformation perpendicular to the PZT patch surface. Therefore, it is necessary to apply the displacements obtained from PZT SA model when modeling the ultrasonic wave propagation.

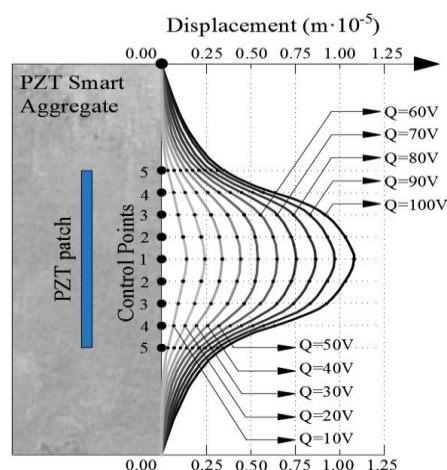


Figure 6. Displacement curves for different electric charge

It should be noted, that results based on numerical simulations of PZT smart aggregates require experimental verification. In case of not matching of the results from experimental analysis and numerical simulation, it is necessary to calibrate the numerical model.

## 5. CONCLUSION

Piezoelectric Smart Aggregates are multifunctional sensors/actuators having wide application in damage detection of reinforced concrete structures. Their application so far is based on performed experimental studies. Numerical models of PZT SA are very rarely analyzed and can be found in a small number of papers. This paper presents the numerical modeling procedure for PZT SA using the ABAQUS/STANDARD software package. Based on the FEM model, deformation-electric voltage curves were obtained for the analyzed voltages in the 10V-100V range with a step of 10V. A linear relationship between deformation and electrical voltage at control points was obtained, and nonlinear change of deformation through cross-sectional height. The presented results of displacement of PZT SA can be used for numerical modeling of wave propagation for damage detection purpose.

## REFERENCES

[1] Liu, T., Zou, D., Du, C., and Wang, Y. (2017) „Influence of axial loads on the health monitoring of concrete structures using embedded piezoelectric transducers“, *Structural Health Monitoring*, Vol. 16(2), pp. 202-214.

[2] Chalioris, C., et. al. (2016) „Applications of smart piezoelectric materials in a wireless admittance monitoring system (WiAMS) to Structures –

Tests in RC elements“, *Case Studies in Construction Materials*, vol. 5, pp.1-18.

- [3] Mo, Y.L., Song, G., Moslehy, Y., Gu, H., Sanders, D.H. and Belarbi, D.J. (2011) „Damage Detection of Reinforced Concrete Columns Subjected to Combined Actions“, *NEESR Payload, Annual Report 2010-2011*, University of Houston.
- [4] Dumoulin, C., Karaiskos, G. and Deraemaeker, A. (2013) „Monitoring of crack propagation in reinforced concrete beams using embedded piezoelectric transducers“, *VIII International Conference FraMCoS-8*, 10-14 March 2013, Toledo, Spain.
- [5] Zhao, X., Li, H., Du, D. and Wang, J., (2008) „Concrete Structure Monitoring Based on Built-in Piezoelectric ceramics Transducers“, *Sensors and Smart Structures Technologies for Civil, Mechanical and Aerospace Systems – Proceedings of SPIE*, March 2008.
- [6] Song, G., Gu, H., Mo, Y.L., Hsu, T.T.C. and Dhonde, H. (2007) „Concrete structural health monitoring using embedded piezoceramics transducers“, *Smart Materials and Structures*, vol. 16(4), pp. 959-968.
- [7] Yan, S., et. al. (2009) „Health monitoring of reinforced concrete shear walls using smart aggregates“, *Smart Materials and Structures*, vol. 18, 047001 (6pp).
- [8] Gu, H., et.al. (2010) „Multi-functional smart aggregate-based structural health monitoring of circular reinforced concrete columns subjected to seismic excitations“, *Smart Materials and Structures*, vol. 19, 065026, (7pp).
- [9] Liao, W.I., et.al. (2011) „Structural health monitoring of concrete columns subjected to seismic excitations using piezoceramic-based sensors“, *Smart Materials and Structures*, vol. 20, 125015, (10pp).
- [10] Stojić, D., Nestorović, T., Marković, N., Marjanović, M., (2018) „Experimental and numerical research on damage localization in plate-like concrete structures using hybrid approach“, *Structural Control and Health Monitoring*, Vol. 25, Issue 9.
- [11] Zhang, H., Shuang, H., and Ou, J., (2018) „Validation of Finite Element Model by Smart Aggregate-Based Stress Monitoring“, *Sensors*, Vol. 18, 4062.
- [12] Marković, N., Nestorović, T., Stojić, N., (2015) „Numerical modeling of damage detection on concrete beams using piezoelectric patches“, *Mechanics Research Communications*, vol. 64, pp. 15-22.
- [13] Stojić, D., Nestorović, T., Marković, N., Cvetković, R. (2019) „Material defects localization in concrete plate-like structures – Experimental and numerical study“, *Mechanics Research Communications*, Vol. 98, pp. 9-15.
- [14] Marković, N., et.al.(2015) „Hybrid approach for two dimensional damage localization using piezoelectric smart aggregates“, *Mechanics Research Communications*, vol. 85, pp. 69-75.